Age-related changes in “cortical” 1/f dynamics are explained by cardiac activity

Fabian Schmidt[1]*, Sarah K. Danböck[1], Eugen Trinka[1,2,3], Gianpaolo Demarchi[1], Nathan Weisz[1,2]

[1]Paris-Lodron-University of Salzburg, Department of Psychology, Centre for Cognitive Neuroscience, Salzburg, Austria

[2]Neuroscience Institute, Christian Doppler University Hospital, Paracelsus Medical University, Salzburg, Austria

[3]Department of Neurology, Christian Doppler University Hospital, Paracelsus Medical University, Salzburg, Austria

ABSTRACT

The power of electrophysiologically measured cortical activity decays $1/f^{\chi}$. The slope of this decay (i.e. the spectral exponent) is modulated by various factors such as age, cognitive states or psychiatric/neurological disorders. Interestingly, a mostly parallel line of research has shown similar effects for the spectral exponent in the electrocardiogram (ECG). This raises the question whether these bodywide changes in spectral exponents are independent or if the “cortically” measured decay in power is explained by cardiac activity captured by cortical sensors (via volume conduction). Focusing on well-established age-related changes in spectral exponents, we analyzed a total of 1282 recordings of magnetoencephalography (MEG) resting state measurements with concurrent ECG in an age-diverse sample. We show that age-related changes of the spectral exponent of neural power spectra are largely explained by cardiac activity. Our results raise concerns when interpreting aperiodic activity as “cortical“ in absence of ECG recordings.

INTRODUCTION

Aperiodic neural activity is omnipresent both in invasive (e.g. ECoG (Miller et al., 2009)) and non-invasive (e.g. MEG/EEG (Demanuele et al., 2007; Pritchard, 1992)) recordings of electrophysiological brain activity and even in hemodynamic responses (e.g. fMRI (He et al., 2010)). In the frequency domain, when visualized in log-log coordinates (log-frequency/log-power), aperiodic activity manifests as a linear decay in power with an increase in frequency (Miller et al., 2009). This part of the signal - following a so-called "power-law" distribution - is often referred to as "scale-free", "1/f noise" or more recently "aperiodic neural activity" (Donoghue et al., 2020).

In the past, aperiodic neural activity, other than periodic neural activity (local peaks that rise above the "power-law" distribution), was often treated as noise and simply removed from the signal e.g. via prewhitening (Buzsáki, 2006; Mitra & Pesaran, 1999). However, in recent years the analysis of aperiodic neural activity gained increasing interest. Several studies have shown that aperiodic neural activity is meaningfully modulated by various factors, such as age (Voytek et al., 2015), cognitive state (e.g. awake vs. sleep; (He et al., 2010)) and disorders like Parkinson's disease and epilepsy (Ghinda et al., 2021; Mostile et al., 2019). However, aperiodic activity is not only present in recordings of neural activity, but also part of other physiological signals such as cardiac activity, often measured using electrocardiography (ECG; (Saul et al., 1988)). Interestingly, and mostly overlooked by the neuroscience community, aperiodic activity measured using ECG has also been linked to age (Beckers et al., 2006), cognitive states (eg. awake vs. sleep; (Penzel et al., 2003)) and disorders such as Parkinson's disease and epilepsy (Ansakorpi, 2002; Haapaniemi, 2001).

It is well known that, via volume conduction, cardiac activity can also be captured in invasive and non-invasive recordings of neural activity (Dirlich et al., 1997; Jousmäki & Hari, 1996; Kern et al., 2013). In MEG recordings cardiac activity is routinely measured via ECG and commonly rejected from the signal (Gross et al., 2013). In clinical EEG recordings, e.g. for the diagnosis of epilepsy, the recording of ECG is standard practice. However, in cognitive neuroscience research the influence of cardiac activity on the EEG is often deemed less problematic (Dirlich et al., 1997) and ECG is rarely recorded/reported. This may be problematic as ECG signals recorded at the head can reach amplitudes of ~5-15μV, which is en par with the size of common evoked responses measured using EEG (Haenschel et al., 2007; von Rosenberg et al., 2017).

Given that aperiodic activity in recordings of neural and cardiac activity is modulated by

similar traits, states and disorders, we ask: are these bodywide changes in aperiodic activity independent, or do changes in aperiodic "cortical" activity actually reflect changes in cardiac activity (captured by e.g. M/EEG sensors)? To address this question, we turn our attention to the recently reported (Donoghue et al., 2020; Voytek et al., 2015) and replicated (Merkin et al., 2022) association between aperiodic activity and chronological age. Using the publicly available Cam-CAN dataset (Shafto et al., 2014; Taylor et al., 2017), we find that age-related changes in aperiodic activity, previously attributed to neural activity, are explained by cardiac activity.

RESULTS

Aperiodic signals recorded using ECG are associated with aging

Changes of aperiodic activity in recordings of neural and cardiac activity are associated with aging (Beckers et al., 2006; Voytek et al., 2015). However, analyses of ECG signals - in the frequency domain - typically focus on (a-)periodic signals <0.4Hz (Shaffer & Ginsberg, 2017). These (compared to neural time series) slowly fluctuating signals are related to heart rate variability (Task Force of the European Society of Cardiology the North American Society of Pacing Electrophysiology, 1996). Changes in (a-)periodic activity at these low frequencies are well established physiological measures (Azuaje et al., 2006). While meaningful information of the ECG can be extracted at much higher rates (e.g. ventricular late potentials [80-500Hz]; (Hunt, 2002)) substantially less is known about aperiodic activity above 0.4Hz in the ECG. To understand whether aperiodic activity recorded using ECG carries meaningful information about aging - at frequency ranges common in M/EEG recordings - the ECG data of 4 age-diverse populations with a total of 2286 subjects were analyzed.

After preprocessing (see Methods) age was used to predict the spectral exponent of the ECG. Our results show that the association between age and the spectral exponent increased with the frequency range used to estimate the spectral exponent up to ~145 Hz (in 3 of 4 datasets; see Figure 1A). At a frequency range of 0.5-145 Hz, age correlated negatively with the spectral exponent measured using ECG in Dataset 1 (r = -.39, *HDI*=[-.45, -.31]), Dataset 2 (r = -.40, *HDI*=[-.46, -.32]), Dataset 3 (r = -.35, *HDI*=[-.41, -.27]) and Dataset 4 (r = -.12, *HDI*=[-.19, -.04]) (see Figure 1A). These results show that aperiodic activity

measured via ECG is associated with aging at frequency ranges vastly exceeding those typically investigated via ECG, but overlapping with frequency ranges commonly measured in recordings of neural activity. To understand whether and how the aperiodic ECG signal spanning this broad frequency range also relates to heart rate (variability), we correlated the spectral exponent with common ECG measures. The results show that the spectral exponent relates to several typical measures of heart rate (variability) (see Figure 1B). This suggests that the spectral exponent carries meaningful information about heart rate (variability), even when including high frequency activity.

Importantly, the direction of the association between age and aperiodic ECG activity is identical to that reported for age and aperiodic EEG activity (Donoghue et al., 2020; Voytek et al., 2015), motivating the investigation of these relationships in combined neural and cardiac measurements.

Cardiac activity is directly captured in EEG and MEG recordings

Aperiodic activity recorded using ECG (see Figure 1A) and EEG/ECoG (Voytek et al., 2015) is similarly modulated by age. In most MEG and some EEG recordings cardiac activity is measured via ECG (Gross et al., 2013). Components of the signal related to cardiac activity are then commonly removed (e.g. via ICA (Hyvarinen, 1999)). In recordings of EEG the influence of cardiac activity is often deemed less problematic (Dirlich et al., 1997). As a result ECG is rarely recorded. However, this may be problematic as ECG signals recorded at the head can reach amplitudes of ~5-15μV, which overlaps with the amplitude of evoked responses measured using EEG (Haenschel et al., 2007; von Rosenberg et al., 2017).

We utilized concurrent ECG, EEG and MEG resting state recordings to examine to what extent ECG signals are captured in the signals measured using MEG and EEG. We calculated so-called temporal response functions (see Methods), to detect whether the signals recorded at different locations (M/EEG vs. ECG) are instantaneously related (zero-time-lags; and therefore likely correspond to the same source) or if one lags behind the other (non zero-time-lags; likely different sources influencing each other e.g. via interoception see (Schulz, 2016)). After preprocessing (see Methods) the data was split in three conditions using an independent component analysis (ICA; (Hyvarinen, 1999)). Independent components that were correlated (at $r > 0.4$; see Methods) with the ECG electrode were either not removed from the data (Figure 1CDEF - blue), removed from the

data (Figure 1CDEF - orange) or projected back separately (Figure 1CDEF - green). Afterwards, temporal response functions (encoding models; see Methods) between the signal recorded at the ECG electrode and the MEG/EEG sensors and feature reconstruction models (decoding models) were computed (for each condition respectively). Our results show that if ECG components are not removed via ICA the ECG signal is captured equally strong at zero-time-lags both in EEG and MEG recordings (see Figure 1CEF). Even after removing ECG related components from the data TRF peaks emerged (although reduced) at zero-time-lags in EEG, but not in MEG recordings (see Figure 1CD). Furthermore, reconstruction (decoding) of the ECG signal was reduced, but remained above chance even after rejecting the ICA signal using ECG both in MEG and EEG recordings ($r > 0$). Interestingly, the presence of the ECG signal was more pronounced in EEG compared to MEG recordings, after removing ECG related components ($\beta_{EEG > MEG} = 0.13$, $HDI = [0.065, 0.21]$; Figure 1F). Additionally, ECG related components extracted from MEG recordings were stronger related to the ECG signal than the components extracted from the EEG ($\beta_{EEG > MEG} = -0.15$, $HDI = [-0.28, -0.05]$; Figure 1F). These results show that a) residual ECG activity remains in surface neural recordings, even after applying a sensitive threshold to detect and remove ECG components via ICA and b) neural and cardiac activity are better separable in MEG as opposed to EEG recordings (see Figure 1CDE). This suggests that residual ECG activity (after an ICA) is more pronounced in EEG compared to MEG recordings. Further investigation of the ECG components (green) shows that they are related to the measured ECG signal at zero-time-lags suggesting no neurovascular interaction (e.g. via interoception; see Figure 1CD).

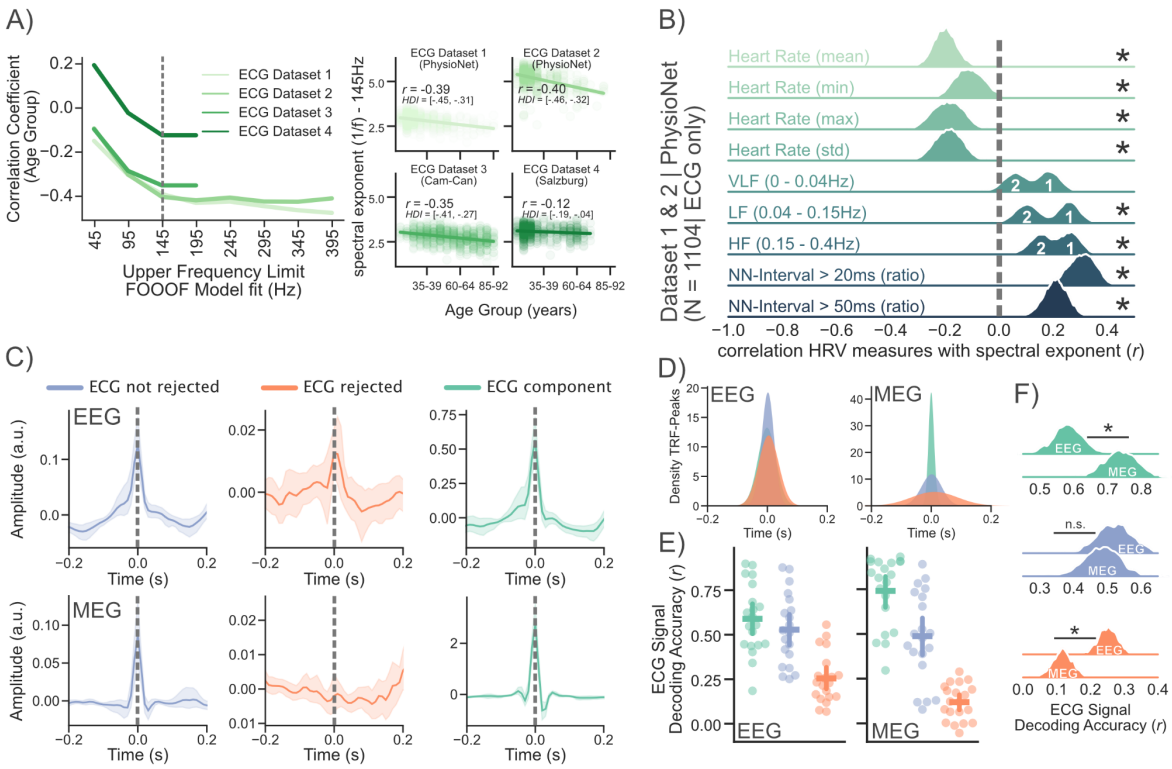

Figure 1: Aperiodic signals recorded using ECG are associated with aging and cardiac activity is captured in EEG and MEG recordings **A)** The spectral exponent recorded using ECG was calculated using different upper frequency limits and correlated with age. This analysis shows that the association between age and spectral exponent increased until ~145 Hz in 3 of 4 datasets. **B)** The spectral exponent of the ECG (fit in a range of 0.5 - 145Hz) was related to common measures of heart rate (variability) **C)/D)** Cardiac activity is captured at zero time lags in concurrent MEG and EEG recordings, if the ECG signal is rejected via ICA this effect disappears in MEG, but not completely in EEG data. **E)/F)** Reconstruction of the ECG signal was impaired, but remained possible even after rejecting the ICA signal using ECG (both in MEG and EEG data). Notably, reconstruction of the ECG signal (after ICA) worked better in EEG than MEG data. A * indicates a "significant" effect i.e. 94% of the highest (probability) density interval (HDI) of the posterior for a given parameter was not overlapping with zero.

Age-related changes in aperiodic brain activity are explained by cardiac components

ECG signals are captured in brain activity recorded using M/EEG (see Figure 1C). Furthermore, aperiodic activity recorded using ECG is - just like aperiodic activity recorded using EEG/ECoG - modulated by age (see Figure 1A). However, it is unclear whether these bodywide changes in aperiodic activity are independent or if "cortically" measured aperiodic activity is explained by cardiac activity captured by cortical sensors (via volume conduction).

To answer this question we are leveraging resting state MEG recordings of an age-diverse population obtained from the Cam-CAN inventory (N = 627; (Shafto et al., 2014; Taylor et al., 2017). After preprocessing (see Methods) an ICA was applied to separate MEG activity from activity related to the ECG. ICA components that were related to the ECG signal were identified using a threshold (r > 0.4; same threshold as in 1CDEF). The data was split in three conditions ($MEG_{ECG\ not\ rejected}$ [blue], $MEG_{ECG\ rejected}$ [orange] and $MEG_{ECG\ component}$ [green]; see Figure 2AB) and projected back to sensor space respectively. Age was then used to predict the spectral exponent averaged across all 102 magnetometers per subject (split by condition). The results show that the spectral exponent increases with age when the ECG signal is not rejected (Figure 2A - blue; $\beta_{standardized}$ = 0.16, HDI = [0.09, 0.24]). Rejecting the ECG signal (Figure 2A - orange) resulted in a strong decrease of the effect of age on the spectral exponent ($\beta_{standardized}$ = 0.08, HDI = [0.01, 0.16]). The probability that the effect of age on the spectral exponent was stronger before removing the ECG component is 92.4% ($\beta_{ECG\ not\ rejected} > \beta_{ECG\ rejected}$). Furthermore, the strongest effect of age on the spectral exponent was found in the data reflecting only the ECG components (green; $\beta_{standardized}$ = 0.31, HDI = [0.24, 0.39]). These results show that most of the age related variance can be explained by the ICA components related to the ECG extracted from the MEG data. Removing ECG components from the data decreases the relationship between age and the spectral exponent. However, a significant relationship with age was still present in our data after rejecting ECG components. This could either be due to residual ECG activity in the MEG signal (see Figure 1EF) or genuine cardiac-related neural activity. To investigate whether $MEG_{ECG\ component}$ and $MEG_{ECG\ rejected}$ explain unique variance in age, a multiple regression model was calculated with $MEG_{ECG\ component}$ and $MEG_{ECG\ rejected}$ as predictors of age (see Figure 2C). This analysis (also visualized as semi-partial correlation coefficients) shows that adding $MEG_{ECG\ component}$ as predictor reduced the relationship between the spectral exponent (without ECG components) and age (see Figure 2C; $\beta_{ECG\ rejected}$ = -2.45, HDI = [-11.88, 6.53]) resulting in a non-significant relationship between $MEG_{ECG\ rejected}$ and age. Whereas the relationship between age and $MEG_{ECG\ Component}$ remained significant ($\beta_{ECG\ rejected}$ = 37.21, HDI = [25.29, 46.36]). This shows that the relationship between age and the spectral exponent, averaged across all MEG sensors, is mostly explained by non-neural activity produced by the heart. Importantly, on average only 1.43 components (SD = 0.68) related to the ECG signal were selected. The low number of extracted components suggests that the reported effects can't be reduced to a general decrease in variance via ICA component selection. To

ensure that the effects shown are not dependent on the ICA thresholds used or the applied $FOOOF_{range}$ the analysis in 2A was also conducted for other thresholds showing a similar pattern (see Supplementary S4 & S5). We further managed to replicate the finding that ECG components are the main contributor to age-related changes in the spectral exponent on resting state recordings (N = 655) obtained as part of MEG studies routinely conducted at the University of Salzburg (see Supplementary S2). Surprisingly, the relationship between age and the spectral exponent in MEG data we found is overall positive, whereas the relationship between age and the spectral exponent extracted from ECG (see Figure 1A) and EEG (Voytek et al., 2015) data is negative. This discrepancy can potentially be explained by scaling differences in spectral exponents between MEG and EEG recordings (Dehghani et al., 2010; He, 2014). These scaling differences are partly general (overall flatter exponents in MEG data) and partly regionally-specific (steeper sloped spectra at vertex in MEG compared to EEG recordings and vice versa at frontal regions). These observations have been related to non-resistive extracellular media (Dehghani et al., 2010) and the space/frequency structure of the recorded activity (Bénar et al., 2019).

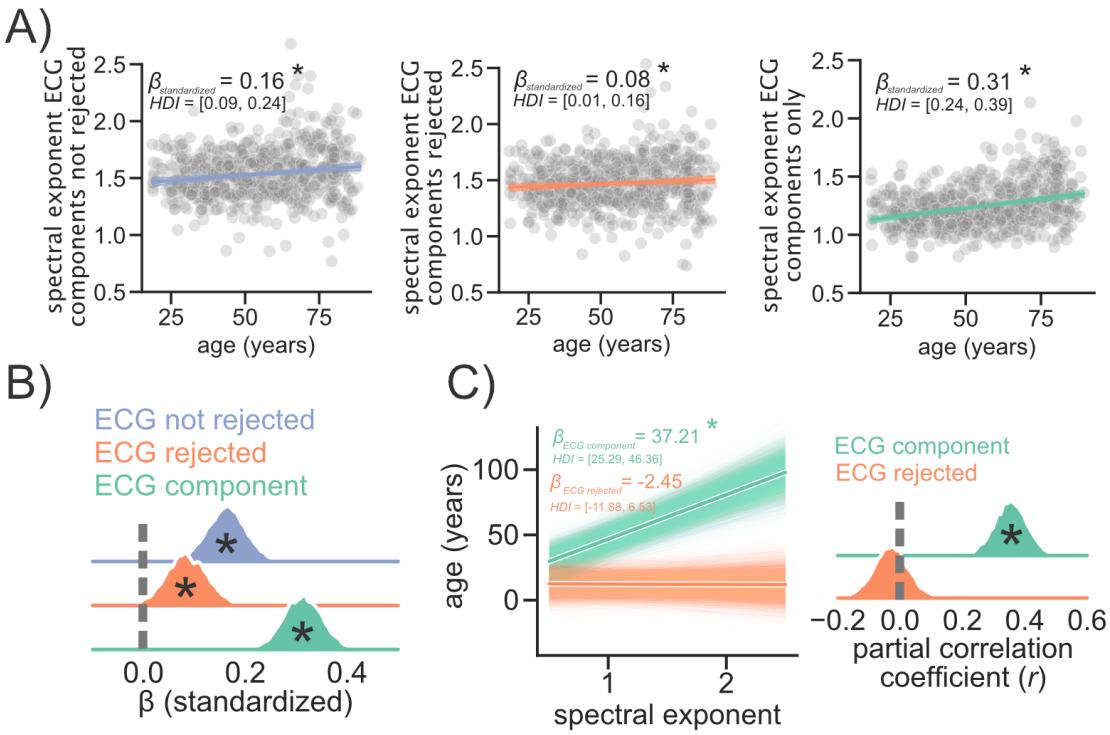

Figure 2: Age-related changes in aperiodic brain activity are explained by cardiac components **A)** Age was used to predict the spectral exponent at rest in three different conditions (ECG components not rejected [blue], ECG components rejected [orange], ECG components only [green]. **B)** Comparison of standardized beta coefficients shows that, while they all exceed zero, the strongest association with age is present on the data reflecting only ECG components **C)** $MEG_{ECG\ rejected}$ and

$MEG_{ECG\ Component}$ were used to predict age. The results of this analysis (also visualized as semi-partial correlations) shows that adding the ECG components as predictor reduced the relationship between the spectral exponent (without ECG components) and age, suggesting that age-related changes in aperiodic brain activity are explained by cardiac components. * indicate a "significant" effect i.e. 94% of the highest (probability) density interval (HDI) of the posterior for a given parameter was not overlapping with zero.

Absence of age-related changes in aperiodic brain activity - at selected channels - when controlling for cardiac activity

So far we have shown that age-related changes in the spectral exponents are explained by activity recorded using ECG (see Figure 2). However, we only showed this effect on the grand average across channels. This analysis ignores potential regional age-related differences in spectral exponents at a subset of channels that might still remain after controlling for contributions from cardiac activity. We therefore repeated the analysis above on single MEG channels (see Figure 3) to see whether genuine cortical effects remain at a subset of channels after controlling for cardiac contributions.

Our results show that, after removing ECG components from the data, age still positively relates ($HDI > 0$) to the spectral exponent at 44 out of 102 channels (see Figure 3A). However, this effect is significantly weaker (decrease in posterior probability > 94%) at 29 out of 102 channels, compared to the condition where the ECG components were not rejected (see Figure 3B). This shows that age still explains some variance in age-related changes of spectral exponents (at certain MEG channels), but the effect of age on spectral exponents is heavily reduced (see Figure 3B). To see if the spectral exponent at channels that are significantly related to age explains unique variance in aging, we averaged the spectral exponent across these channels in the $MEG_{ECG\ rejected}$ and $MEG_{ECG\ component}$ condition respectively. Afterwards a multiple regression model was calculated with $MEG_{ECG\ component}$ and $MEG_{ECG\ rejected}$ as predictors for age (see Figure 3C). This analysis (also visualized via semi-partial correlation coefficients; Figure 3C) reveals that adding $MEG_{ECG\ component}$ as predictor reduces the relationship between the spectral exponent and age (see Figure 3C; $\beta_{ECG\ rejected} = 4.55$, $HDI = [-5.15, 11.83]$) resulting in a non-significant relationship between $MEG_{ECG\ rejected}$ and age. In contrast, the relationship between age and $MEG_{ECG\ Component}$ remained significant ($\beta_{ECG\ rejected} = 37.10$, $HDI = [27.78, 46.93]$), when adding $MEG_{ECG\ rejected}$ as predictor. This suggests that the relationship between age and the spectral exponent, even

at sensors that were still related to age after ECG component rejection (see Figure 3A), is mostly explained by independent components related to the signal recorded using ECG.

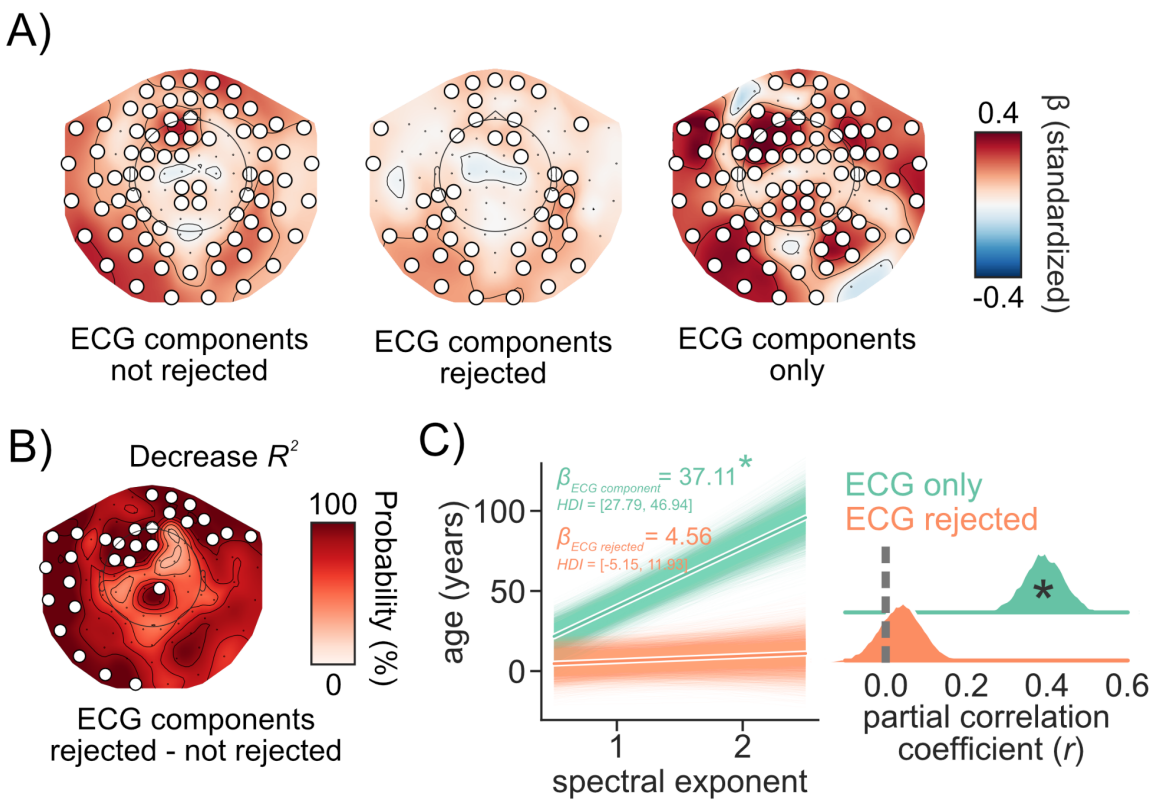

Figure 3: Absence of age-related changes in aperiodic brain activity - at selected channels - when controlling for cardiac activity **A)** Age was used to predict the spectral exponent at rest in three different conditions per channel (ECG components not rejected, ECG components rejected and ECG components only). **B)** Probability that R^2 is higher, if ECG components are not rejected (($R^2_{ECG\ not\ rejected} > R^2_{ECG\ rejected}$) **C)** $MEG_{ECG\ rejected}$ and $MEG_{ECG\ Component}$ were used to predict age. The results of this analysis (also visualized as semi-partial correlations) shows that adding the ECG components as predictor reduced the relationship between the spectral exponent (without ECG components) and age, suggesting that age-related changes in aperiodic brain activity are explained by cardiac components. * indicate a "significant" effect i.e. 94% of the highest (probability) density interval (HDI) of the posterior for a given parameter was not overlapping with zero.

DISCUSSION

Cardiac and cortical recordings of aperiodic electrophysiological signals are related to age (Beckers et al., 2006; Voytek et al., 2015), cognitive states (eg. awake vs. sleep; (He et al., 2010; Penzel et al., 2003)) and disorders such as Parkinson's disease and epilepsy (Ansakorpi, 2002; Ghinda et al., 2021; Haapaniemi, 2001; Mostile et al., 2019). In the present study we investigated the question whether age-related changes in neural and

cardiac aperiodic activity are modulated independently or if “cortically” measured aperiodic activity is explained by cardiac activity captured by surface electrodes (via volume conduction). Our results suggest that cardiac activity explains age-related changes in aperiodic “cortical” activity.

Aperiodic processes are ubiquitous in nature (Gisiger, 2001). They can be observed not only in physiological recordings but are also found in earthquakes, economics, ecology, epidemics, speech, and music (Bak et al., 1987; Gisiger, 2001). In measurements containing multiple aperiodic signals, aperiodic signals might even influence each other (e.g. neural speech tracking; (Schmidt et al., 2021)). Understanding the generative process underlying aperiodic signals is therefore crucial to correctly attribute functional changes to the right source. While our findings suggest that age-related changes in aperiodic signals recorded “cortically” can be attributed to cardiac activity, an aperiodic signal was still present in the data after rejecting ECG related components (see Figure 2A). This suggests that it is unlikely that aperiodic activity related to the ECG explains all facets of aperiodic neural activity (although some ECG related activity was likely still present in the data; see Figure 1EF). However, the age-related modulation of aperiodic activity vastly decreased after rejecting ECG related components (see Figure 2B, 3B) and even disappeared when adding the ECG components as a covariate to the model (see Figure 2C, 3C). The latter shows that neural aperiodic activity does not hold any significant explanatory value beyond cardiac aperiodic activity related to chronological age. These results do not negate the general possibility for the occurrence of independent bodywide changes in aperiodic activity. However, they suggest that independent bodywide changes in aperiodic activity are an unlikely explanation for age-related aperiodic activity. We therefore interpret our results in the direction that age-related changes in cardiac activity explain age-related changes in aperiodic activity recorded via M/EEG. Not considering these artifactual contributions could lead to misinterpretation of age-related effects being of neural origin.

Neural and vascular processes are known to interact with each other (Takarada-Iemata et al., 2019). As vascular processes are also known to change with aging (Tsvetanov et al., 2015) they are a major confound in measures of neural activity that rely on hemodynamic responses and need to be accounted for (e.g. fMRI; (Geerligs et al., 2017)). Cardiovascular activity, in the form of the ECG, is also captured in M/EEG recordings (via volume conduction; see Figure 1CDEF). Our results show that age-related changes in cardiac

aperiodic activity explain age-related changes in “cortical” aperiodic activity (see Figure 2BC & 3BC). Whether these age-related changes in aperiodic cardiac activity can in turn be predicted by longitudinal changes in neural or vascular processes is an exciting research question. This could be investigated in future studies utilizing longitudinal recordings of cardiac and neural activity. In the present study, ECG related components are unlikely to reflect neuro-cardiac interactions, given the sharp clustering of TRF peaks around zero-time-lags (see Figure 1D) suggesting that $MEG_{ECG\ components}$ instantaneously capture $ECG_{measured}$. However, TRF peaks are more widespread around zero-time-lags in the $MEG_{ECG\ rejected}$ condition. This could either hint at genuine neuro-cardiac interactions or simply reflect noisy model fits given the low-amplitude of the TRF (see Figure 1C).

Our results clearly suggest not to overinterpret aperiodic activity recorded from MEG in absence of ECG recordings. We further hypothesize that this may also affect recent investigations of aging and aperiodic activity using EEG (Donoghue et al., 2020; Merkin et al., 2022; Voytek et al., 2015). While artifacts related to cardiac activity are a well-known problem in recordings of MEG activity, this issue has been deemed less problematic in recordings of EEG (Dirlich et al., 1997). However, our data suggests that the ECG signal is captured equally strong in concurrent MEG and EEG recordings (see Figure 1CEF). Furthermore, separating ECG related components from neural activity using ICA seems to work worse in EEG compared to MEG recordings (see Figure 1EF). Therefore, our results suggest that ECG recordings should become more standard practice in EEG research, especially when investigating aperiodic activity to better delineate cardiac and neural contributions. Additionally, further method development is needed to diminish the artefactual impact of cardiac activity on M/EEG recordings.

Delineating cardiac from neural contributions to aperiodic activity is crucial to also improve our understanding of the generative process underlying genuine neural aperiodic activity. For example a current interesting hypothesis states that the generative process underlying aperiodic neural activity is mainly attributed to differences in the ratio between excitatory (AMPA) and inhibitory (GABA) currents, that influence the spectral exponent of the neural power spectrum (Gao et al., 2017). Excitatory currents such as AMPA have a fast decay constant, whereas inhibitory currents like GABA decay more slowly as a function of frequency. This means that flatter power spectra (lower spectral exponents) may be indicative for the presence of more excitatory than inhibitory currents and vice versa

(steeper sloped power spectra; see (Gao et al., 2017)). This theory is (in part) based on research showing that GABAergic drugs like propofol (Gao et al., 2017) and Glutamatergic drugs like ketamine (Waschke et al., 2021) modulate the spectral exponent of electrophysiologically measured power spectra. However, propofol and ketamine not only influence neural activity, but also influence heart rate variability (a core component of the ECG; (Goddard et al., 2021; Kanaya et al., 2003)). So are drug induced effects on the spectral exponent of the power spectrum (measured using surface electrodes) conflated by cardiac artifacts? Previous work showed that propofol induced changes to the spectral exponent were still present in EEG recordings after using ICA to reject ECG components from the data (Lendner et al., 2020). However, our results suggest that cardiac activity remains in EEG signals even after doing an ICA (see Figure 1CEF). It is therefore very plausible that drug induced effects on aperiodic "neural" activity are still conflated by cardiac activity. Future work is needed to see to what extent drug induced changes in aperiodic neural activity can also be attributed to ECG signals. Similar caveats adhere to other findings of functional modulations in aperiodic signals in cognitive states (eg. awake vs. sleep; (He et al., 2010; Penzel et al., 2003)) and disorders like Parkinson's disease and epilepsy (Ansakorpi, 2002; Ghinda et al., 2021; Haapaniemi, 2001; Mostile et al., 2019). While the present analysis focuses on aperiodic activity, our results might also translate to older findings focusing on "presumably" periodic neural activity in canonical frequency bands (e.g. delta, theta, alpha). Until recently aperiodic activity was often discarded as noise. Recently developed algorithms have opened up possibilities to separately analyze aperiodic and periodic activity (Donoghue et al., 2020; Wen & Liu, 2016). This has for instance revealed that previously suspected periodic age-related changes in alpha power are actually attributable to differences in aperiodic activity (Donoghue et al., 2020; Merkin et al., 2022). As we have shown that age-related changes in aperiodic activity are explained by cardiac activity it is possible that our results also translate to previous studies conflating periodic and aperiodic activity.

To conclude: The present study, focusing on age-related changes in aperiodic neural and cardiac activity, suggests that functional changes in aperiodic neural activity might be explained by cardiac activity. Conflating cardiac and neural contributions to (a-)periodic activity obstructs our understanding of genuine neural aperiodic processes and should be avoided. This highlights the need for concurrent recordings of cardiac and neural activity to

further increase our understanding of neural aperiodic activity and its association with age, cognitive states and disorders.

METHODS

Sample

The present study builds on resting-state data from several sources. ECG Dataset 1 & 2 were obtained from PhysioNet (Goldberger et al., 2000) containing 1121 healthy volunteers between 18 to 92 years (divided in 15 age groups for anonymization purposes) (Schumann & Bär, 2021). The MEG data analyzed in this study was obtained from two different sources: the Cam-CAN repository (main manuscript; (Shafto et al., 2014; Taylor et al., 2017)) and resting-state data routinely recorded at the University of Salzburg (Supplementary S3). The sample obtained from Cam-CAN contained 655 healthy volunteers with an age range between 18 and 88 years with an average of 54 and a standard deviation of 18 years. The sample obtained from the University of Salzburg contained 684 healthy volunteers with an age range between 18 and 73 years with an average of 32 and a standard deviation of 14 years. Notably the age distribution recorded at the University of Salzburg was bimodal (with 423 subjects being below 30 the sample is not really reflective of an age-diverse population; see Supplementary S2). For the ECG data no specific criteria for exclusion of participants was applied. In case of the MEG/EEG data participants were excluded when no independent heart component equal or above the threshold was found ($r > 0.4$; see MEG/EEG Processing|Preprocessing). Furthermore, when the automated processing procedure resulted in errors, data was considered as missing. This resulted in a total of 1104 ECG recordings from PhysioNet, 627 MEG recordings from Cam-CAN and 655 MEG recordings from the University of Salzburg.

Statistical Inference

To investigate the relationship between e.g. age and aperiodic activity recorded using MEG, we used bayesian generalized linear models (GLMs) either build directly in PyMC (a python package for probabilistic programming; (Salvatier et al., 2016)) or in Bambi (a high-level interface to PyMC; (Capretto et al., 2022)). Decisions for either Bambi or PyMC were made based on the accessibility of appropriate statistical families for the respective dependent variables in a GLM. Priors were chosen to be weakly informative (exact prior specifications for each model can be obtained from the code in the corresponding authors github repository; see Data and Code availability). Results were considered of “statistical significance”, if 94% of the highest (probability) density interval (HDI) of the posterior for a

given *β-coefficient* was not overlapping with zero. Further, it was ensured that for all models there were no divergent transitions ($R_{hat} < 1.05$ for all relevant parameters) and an effective sample size > 400 (an exhaustive summary of bayesian model diagnostics can be found in (Vehtari et al., 2021)).

MEG/EEG Processing

MEG/EEG Processing - Data acquisition

MEG data (Cam-CAN; Figure 2 & 3) was recorded at the University of Cambridge, using a 306 VectorView system (Elekta Neuromag, Helsinki). MEG data (Salzburg; Figure 1C & Supplementary S2 and S3) was recorded at the University of Salzburg, using a 306 channel TRIUX system (MEGIN Oy, Helsinki). Both systems are equipped with 102 magnetometers and 204 planar gradiometers and positioned in magnetically shielded rooms. In order to facilitate offline artifact correction, electrooculogram (VEOG, HEOG) as well as ECG was measured continuously in both recording sites. In a subset of the Salzburg recordings EEG was measured additionally (see Figure 1) using a 32-channel system provided by the MEG manufacturer. Data recorded at Cambridge was online filtered at 0.03-1000 Hz, whereas data recorded at Salzburg was online filtered at 0.1-333 Hz with a 1000 Hz sampling rate at both recording sites. Four (Cambridge) and five (Salzburg) Head-Position Indicator coils were used to measure the position of the head. All data used in the present study contains passive resting-state measurements lasting about ~8min (Cambridge) and ~5min (Salzburg). Further data processing at both recording sites was conducted similarly and will therefore be reported together.

MEG/EEG Processing - Preprocessing

Initially, a Signal-Space-Separation (SSS; (Taulu & Kajola, 2005; Taulu & Simola, 2006)) algorithm was used to find and repair bad channels (implemented in MNE-Python *version 1.2*; (Gramfort, 2013)). Afterwards the data was high-pass filtered at 0.1Hz using a finite impulse response (FIR) filter (Hamming window). For extracting physiological “artifacts” from the data, 50 independent components were calculated using the *fastica* algorithm ((Hyvarinen, 1999); implemented in MNE-Python *version 1.2*; note: 50 components were selected for MEG for computational reasons for the analysis of EEG data no threshold was applied). As ICA is sensitive to low-frequency drifts independent components were calculated on a copy of the data high-pass filtered at 1Hz. Components related to cardiac

and ocular activity were determined via correlation with concurrent ECG, VEOG and HEOG recordings. A threshold of $r > 0.4$ was applied to detect the ECG components and a threshold $r > 0.8$ for detecting EOG components in the data. The more sensitive threshold used for ECG component detection was decided upon based on the strong presence of ECG signals in resting state M/EEG recordings (see Figure 1C). The computed ICA was then applied to the original data, either rejecting all components apart from those related to the ECG, or rejecting only EOG related components, or ECG and EOG related components. This resulted in three conditions $MEG_{ECG\ not\ rejected}$, $MEG_{ECG\ rejected}$ and $MEG_{ECG\ component}$. The data was then split in 2 second epochs and residual artifacts were determined using an adaptive and automatic artifact detection method (the "Riemannian Potato" implemented in pyriemann; (Barachant et al., 2013)). Epochs were rejected when the covariance matrix of an epoch differed by >2.5 standard deviations from a centroid covariance matrix.

MEG/EEG Processing - Temporal Response Functions

To estimate the extent at which ECG activity is captured by MEG/EEG recordings, we calculated temporal response functions (TRFs). In brief, the assumption behind a TRF is that a dependent variable is the result of a (or several) predictor variables. This approach can be used to model a time-series as a linear function of one (or several) time series and can be formulated (for a single predictor; see (Brodbeck et al., 2021)) as:

$$y_t = \sum_{\tau=\tau_{min}}^{\tau_{max}} h_\tau x_{t-\tau}$$

Where h represents the TRF, also sometimes described as filter kernel, and τ represents potential delays between y and x (for an extensive explanation of the algorithm used herein see (Brodbeck et al., 2021)). Typically, this approach is used to estimate spectro-temporal receptive fields, e.g. in response to auditory stimuli (David et al., 2007), where the interpretation of a TRF follows that of an ERP/F in response to a continuous input signal (Lalor et al., 2006). This model can be used as a forward or encoding model to predict the brain response from a stimulus representation or as a backward or decoding model to reconstruct a stimulus representation from brain recordings. We used this approach here to detect whether signals recorded at different locations interact with each other. Forward and Backward models were calculated between the M/EEG signal and the signal recorded using

ECG. This was done to see if signals measured using M/EEG and ECG follow/precede each other (non zero-time lags; e.g. via interoception see (Schulz, 2016)) or if the signals are instantaneously related (zero-time-lags; therefore likely corresponding to the same underlying signal source). As computations of TRFs are quite memory and time extensive, the MEG, EEG and ECG data was additionally low pass filtered at 45Hz (to avoid aliasing) and downsampled to 100Hz before the analysis (a common practice when computing TRFs; see (Brodbeck et al., 2021)). The TRF time courses visualized in Figure 1C were obtained by computing a principle component analysis (PCA; (Pearson, 1901)) within subject and across all channels, whereas the distribution of peaks visualized in Figure 1D was obtained by calculating the RMS across channels and extracting the maximum value.

MEG/EEG Processing - Spectral analysis

Power spectra were computed using Welch's method (Welch, 1967) implemented in *neurodsp* (Cole et al., 2019) between 0.5 and 145Hz (0.5 Hz resolution). Afterwards the spectral parameterization algorithm (implemented in *FOOOF* version 1.0.0; (Donoghue et al., 2020)) was used to parametrize the power spectra. Power spectra were parameterized across a frequency range of 0.5–145 Hz. The maximum number of peaks was set to zero (for computational reasons). The aperiodic mode was left at 'fixed' given that power spectra (on average) showed a linear decay in log-log coordinates (see Supplementary S1).

ECG Processing

The ECG data recorded as part of the MEG recordings was processed alongside the MEG data. Therefore the preprocessing and spectral analysis settings from the section "MEG/EEG Processing" apply also to the ECG part of dataset 3 & 4 (see Figure 1). Below ECG processing for the data obtained from PhysioNet is described. The processing differed in parts, to better relate classical measures of heart rate (variability) (HRV) to aperiodic cardiac activity.

ECG Processing - Data acquisition and HRV analysis

The ECG data obtained from PhysioNet was acquired at the Jena university hospital (Schumann & Bär, 2021). The study was approved by the ethics committee of the Medical Faculty of the Friedrich Schiller University Jena. All research was performed in accordance with relevant guidelines and regulations. The informed written consent was obtained from

all subjects. ECG data was recorded at a sampling rate of 1000 Hz using one of two different recording devices. Either an MP150 (ECG100C, BIOPAC systems inc., Golata, CA, USA) or a Task Force Monitor system (CNSystems Medizintechnik GmbH, Graz AUT). More detailled information about the ECG recordings can be obtained from https://physionet.org/content/autonomic-aging-cardiovascular/1.0.0/. The data was either further analyzed using spectral analysis (as above) or standard HRV parameters were estimated using the open-source toolbox pyHRV (Gomes et al., 2019).

ECG Processing - Spectral analysis

Power spectra were computed using Welch's method (Welch, 1967) implemented in *neurodsp* (Cole et al., 2019) between 0.01 and 145Hz (0.01 Hz resolution). Afterwards the spectral parameterization algorithm (implemented in *FOOOF* version 1.0.0; (Donoghue et al., 2020)) was used to parametrize the power spectra. Power spectra were parameterized across a frequency range of 0.01–145 Hz. The maximum number of peaks was set to zero (for computational reasons). The aperiodic mode was once set to 'knee' given that the power spectra (on average) showed a clear 'knee' in log-log coordinates (see Supplementary S2) and once to better relate the aperiodic parameters of the pure ECG signal to those of the ECG components the data was also parametrized in 'fixed' mode without a knee (see Figure 1).

Data and Code availability

The data analyzed in the main manuscript are mostly obtained from open data sources. The ECG data (Dataset 1 & 2; Figure 1) is obtained from https://physionet.org/content/autonomic-aging-cardiovascular/1.0.0. The MEG/EEG dataset (Figure 1) was obtained at the University of Salzburg as part of routine resting state MEG recordings and is available upon request. The data for the MEG analysis in the main manuscript (Figure 2 & 3) are obtained from the Cam-CAN repository https://www.cam-can.org/index.php?content=functional. All code used for the analysis is publicly available on GitHub at https://github.com/schmidtfa/cardiac_1_f.

Acknowledgements

The authors thank Freek van Ede, Tzvetan Popov, Rik Henson and Kamen Tsvetanov for helpful comments and discussions and Thomas Hartmann for a code review. Sarah K. Danböck was supported by the Doctoral College 'Imaging the Mind' of the Austrian Science Fund (FWF; W1233-B; Subproject Principal Investigator: Frank H. Wilhelm). No specific funding was acquired for this project. The authors declare no conflicts of interest.

Author contributions

Conceptualization: FS, NW

Formal Analysis: FS, SKD

Investigation: FS

Methodology: FS, GD

Software: FS

Supervision: NW, GD

Visualization: FS

Writing—original draft: FS

Writing—review & editing: FS, SKD, ET, NW, GD

SUPPLEMENTARY MATERIAL

Supplementary S1:

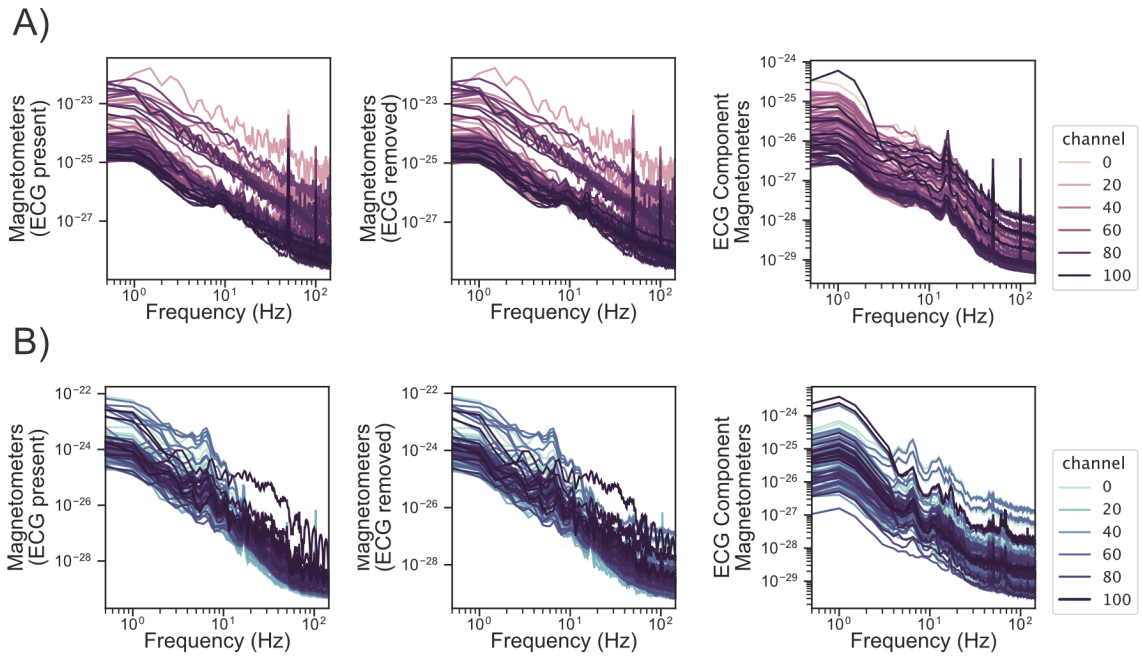

Supplementary S1: Grand average power spectra for the MEG data recorded at **A)** Cambridge and **B)** Salzburg split in the three conditions $MEG_{ECG\ not\ rejected}$, $MEG_{ECG\ rejected}$, $MEG_{ECG\ components}$. Given the roughly linear decay in power with frequency, models were fitted using the 'fixed' mode in the FOOOF toolbox (Donoghue et al., 2020).

Supplementary S2:

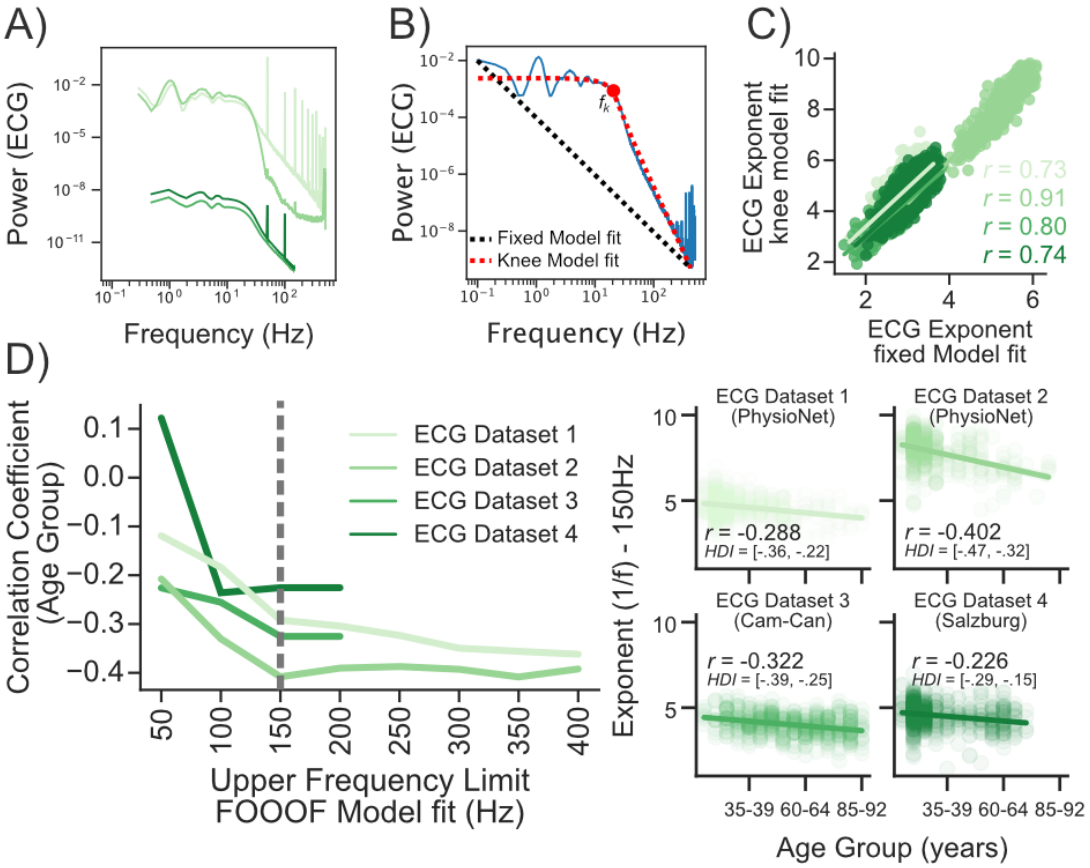

Supplementary S2: ECG power spectra in relation to age **A)** grand average power spectra plotted separately per Dataset **B)** Schematic illustrating the differences between fixed and knee model fits. In the main main part of the manuscript "fixed" model fits were used for better comparability with the "fixed" model fits in MEG data although "knee" fits better describe the pure ECG spectra. **C)** Comparison of knee and fixed model fits shows that both are strongly correlated. **D)** The spectral exponent recorded using ECG was calculated using different upper frequency limits and correlated with age. This analysis shows that the association between age and spectral exponent increased until ~145Hz in 3 of 4 datasets. Similarly, as in Figure 1A when using "fixed" model fits.

Supplementary S3:

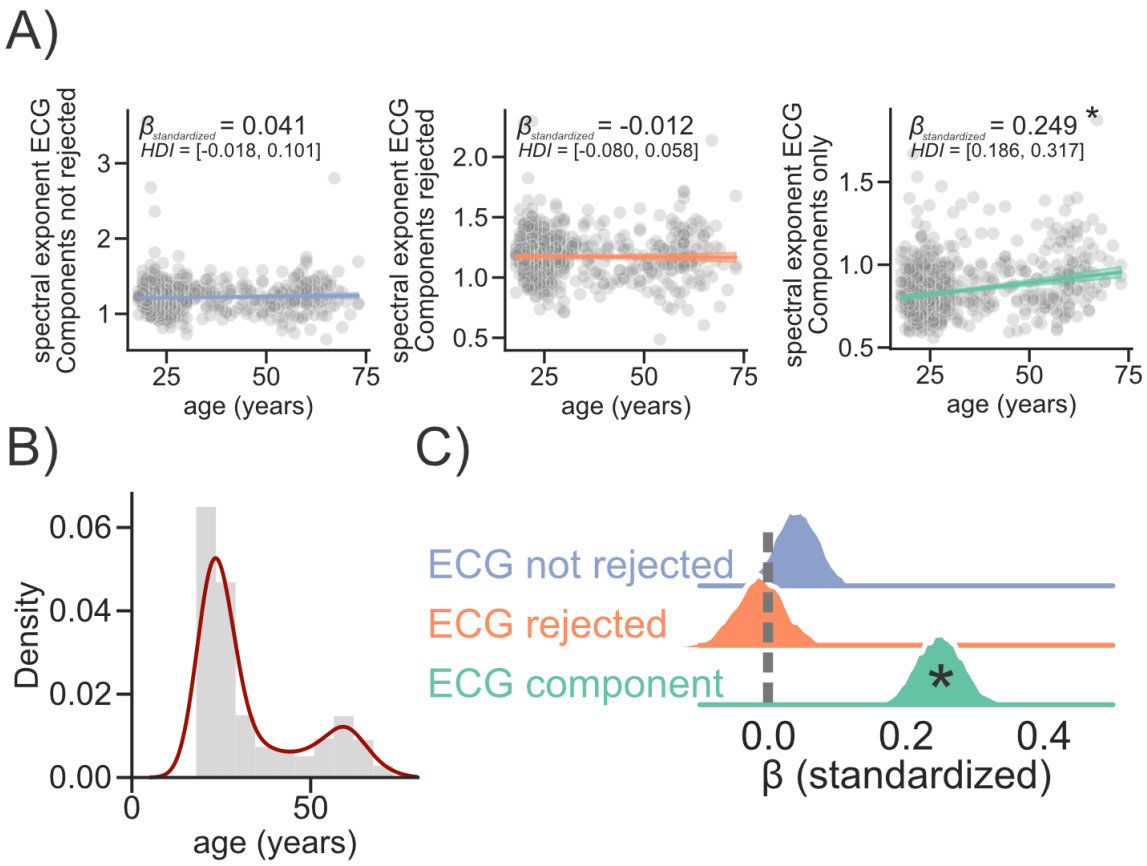

Supplementary S3: Age-related changes in aperiodic brain activity are explained by cardiac components **A)** Age was used to predict the spectral exponent at rest in three different conditions (ECG components not rejected [blue], ECG components rejected [orange], ECG components only [green]. **B)** Age distribution in the sample routinely recorded as part of MEG measurements at the University of Salzburg. **C)** Comparison of standardized beta coefficients shows that the strongest and only association with age is present on the data reflecting only ECG components * indicate a "significant" effect i.e. 94% of the highest (probability) density interval (HDI) of the posterior for a given parameter was not overlapping with zero.

Supplementary S4:

Table 1: age-related changes in spectral exponent (using different ICA thresholds)

	$\beta_{standardized}$	hdi 3%	hdi 97%
ICA Threshold $r > 0.4$ ($N = 627$)			
$MEG_{ECG\ not\ rejected} \sim 1 + age$	0.163*	0.092	0.235
$MEG_{ECG\ rejected} \sim 1 + age$	0.084*	0.013	0.163
$MEG_{ECG\ component} \sim 1 + age$	0.313*	0.244	0.387
ICA Threshold $r > 0.5$ ($N = 597$)			
$MEG_{ECG\ not\ rejected} \sim 1 + age$	0.174*	0.102	0.247
$MEG_{ECG\ rejected} \sim 1 + age$	0.099*	0.028	0.176
$MEG_{ECG\ component} \sim 1 + age$	0.316*	0.245	0.390
ICA Threshold $r > 0.6$ ($N = 537$)			
$MEG_{ECG\ not\ rejected} \sim 1 + age$	0.165*	0.082	0.243
$MEG_{ECG\ rejected} \sim 1 + age$	0.089*	0.009	0.173
$MEG_{ECG\ component} \sim 1 + age$	0.308*	0.232	0.388
ICA Threshold $r > 0.7$ ($N = 464$)			
$MEG_{ECG\ not\ rejected} \sim 1 + age$	0.157*	0.070	0.240
$MEG_{ECG\ rejected} \sim 1 + age$	0.084	-0.003	0.172
$MEG_{ECG\ component} \sim 1 + age$	0.309*	0.221	0.389
ICA Threshold $r > 0.8$ ($N = 276$)			
$MEG_{ECG\ not\ rejected} \sim 1 + age$	0.138*	0.028	0.249
$MEG_{ECG\ rejected} \sim 1 + age$	0.075	-0.034	0.185
$MEG_{ECG\ component} \sim 1 + age$	0.316*	0.202	0.427

Note: Dependent Variable = spectral exponent; * indicate “significant” effects

Supplementary S5:

Table 1: age-related changes in spectral exponent (using different $FOOOF_{ranges}$)

	$\beta_{standardized}$	hdi 3%	hdi 97%
$FOOOF_{range}$ (0.5 - 45Hz) & ICA Threshold $r > 0.4$			
$MEG_{ECG\ not\ rejected}$ ~ 1 + age	0.018	-0.030	0.064
$MEG_{ECG\ rejected}$ ~ 1 + age	-0.032	-0.084	0.023
$MEG_{ECG\ component}$ ~ 1 + age	0.104*	0.045	0.159
$FOOOF_{range}$ (0.5 - 95Hz) & ICA Threshold $r > 0.4$			
$MEG_{ECG\ not\ rejected}$ ~ 1 + age	0.160*	0.094	0.230
$MEG_{ECG\ rejected}$ ~ 1 + age	0.091*	0.017	0.162
$MEG_{ECG\ component}$ ~ 1 + age	0.293*	0.227	0.369
$FOOOF_{range}$ (0.5 - 145Hz) & ICA Threshold $r > 0.4$			
$MEG_{ECG\ not\ rejected}$ ~ 1 + age	0.163*	0.092	0.235
$MEG_{ECG\ rejected}$ ~ 1 + age	0.084*	0.013	0.163
$MEG_{ECG\ component}$ ~ 1 + age	0.313*	0.244	0.387

Note: Dependent Variable = spectral exponent; * indicate “significant” effects

REFERENCES

Ansakorpi, H. (2002). Heart rate dynamics in refractory and well controlled temporal lobe epilepsy. *Journal of Neurology, Neurosurgery & Psychiatry*, *72*(1), 26–30. https://doi.org/10.1136/jnnp.72.1.26

Azuaje, F., Clifford, G., & McSharry, P. (2006). *Advanced Methods and Tools for ECG Data Analysis*. Artech.

Bak, P., Tang, C., & Wiesenfeld, K. (1987). Self-organized criticality: An explanation of the 1/*f* noise. *Physical Review Letters*, *59*(4), 381–384. https://doi.org/10.1103/PhysRevLett.59.381

Barachant, A., Andreev, A., & Congedo, M. (2013). The Riemannian Potato: An automatic and adaptive artifact detection method for online experiments using Riemannian geometry. *TOBI Workshop VI*, 19–20. https://doi.org/hal-00781701

Beckers, F., Verheyden, B., & Aubert, A. E. (2006). Aging and nonlinear heart rate control in a healthy population. *American Journal of Physiology-Heart and Circulatory Physiology*, *290*(6), H2560–H2570. https://doi.org/10.1152/ajpheart.00903.2005

Bénar, C. . G., Grova, C., Jirsa, V. K., & Lina, J. M. (2019). Differences in MEG and EEG power-law scaling explained by a coupling between spatial coherence and frequency: A simulation study. *Journal of Computational Neuroscience*, *47*(1), 31–41. https://doi.org/10.1007/s10827-019-00721-9

Brodbeck, C., Das, P., Kulasingham, J. P., Bhattasali, S., Gaston, P., Resnik, P., & Simon, J. Z. (2021). *Eelbrain: A Python toolkit for time-continuous analysis with temporal response functions* [Preprint]. Neuroscience. https://doi.org/10.1101/2021.08.01.454687

Buzsáki, G. (2006). *Rhythms of the Brain*. Oxford University Press.

https://doi.org/10.1093/acprof:oso/9780195301069.001.0001

Capretto, T., Piho, C., Kumar, R., Westfall, J., Yarkoni, T., & Martin, O. A. (2022). *Bambi: A simple interface for fitting Bayesian linear models in Python* (arXiv:2012.10754). arXiv. http://arxiv.org/abs/2012.10754

Cole, S., Donoghue, T., Gao, R., & Voytek, B. (2019). NeuroDSP: A package for neural digital signal processing. *Journal of Open Source Software*, *4*(36), 1272. https://doi.org/10.21105/joss.01272

David, S. V., Mesgarani, N., & Shamma, S. A. (2007). Estimating sparse spectro-temporal receptive fields with natural stimuli. *Network: Computation in Neural Systems*, *18*(3), 191–212. https://doi.org/10.1080/09548980701609235

Dehghani, N., Bédard, C., Cash, S. S., Halgren, E., & Destexhe, A. (2010). Comparative power spectral analysis of simultaneous elecroencephalographic and magnetoencephalographic recordings in humans suggests non-resistive extracellular media. *Journal of Computational Neuroscience*, *29*(3), 405–421. https://doi.org/10.1007/s10827-010-0263-2

Demanuele, C., James, C. J., & Sonuga-Barke, E. J. (2007). Distinguishing low frequency oscillations within the 1/f spectral behaviour of electromagnetic brain signals. *Behavioral and Brain Functions*, *3*(1), 62. https://doi.org/10.1186/1744-9081-3-62

Dirlich, G., Vogl, L., Plaschke, M., & Strian, F. (1997). Cardiac field effects on the EEG. *Electroencephalography and Clinical Neurophysiology*, *102*(4), 307–315. https://doi.org/10.1016/S0013-4694(96)96506-2

Donoghue, T., Haller, M., Peterson, E. J., Varma, P., Sebastian, P., Gao, R., Noto, T., Lara, A. H., Wallis, J. D., Knight, R. T., Shestyuk, A., & Voytek, B. (2020). Parameterizing neural power spectra into periodic and aperiodic components. *Nature Neuroscience*, *23*(12), 1655–1665. https://doi.org/10.1038/s41593-020-00744-x

Gao, R., Peterson, E. J., & Voytek, B. (2017). Inferring synaptic excitation/inhibition balance from field potentials. *NeuroImage*, *158*, 70–78. https://doi.org/10.1016/j.neuroimage.2017.06.078

Geerligs, L., Tsvetanov, K. A., Cam-CAN, & Henson, R. N. (2017). Challenges in measuring individual differences in functional connectivity using fMRI: The case of healthy aging: Measuring Individual Differences Using fMRI. *Human Brain Mapping*, *38*(8), 4125–4156. https://doi.org/10.1002/hbm.23653

Ghinda, D. C., Lambert, B., Lu, J., Jiang, N., Tsai, E., Sachs, A., Wu, J.-S., & Northoff, G. (2021). Scale-Free Analysis of Intraoperative ECoG During Awake Craniotomy for Glioma. *Frontiers in Oncology*, *10*, 625474. https://doi.org/10.3389/fonc.2020.625474

Gisiger, T. (2001). Scale invariance in biology: Coincidence or footprint of a universal mechanism? *Biological Reviews of the Cambridge Philosophical Society*, *76*(2), 161–209. https://doi.org/10.1017/S1464793101005607

Goddard, K., Sampson, C., Bedy, S.-M., Ghadban, R., & Stilley, J. (2021). Effect of Ketamine on Cardiovascular Function During Procedural Sedation of Adults. *Cureus*. https://doi.org/10.7759/cureus.14228

Goldberger, A. L., Amaral, L. A. N., Glass, L., Hausdorff, J. M., Ivanov, P. Ch., Mark, R. G., Mietus, J. E., Moody, G. B., Peng, C.-K., & Stanley, H. E. (2000). PhysioBank, PhysioToolkit, and PhysioNet: Components of a New Research Resource for Complex Physiologic Signals. *Circulation*, *101*(23). https://doi.org/10.1161/01.CIR.101.23.e215

Gomes, P., Margaritoff, P., & Plácido da Silva, H. (2019). PyHRV: Development and Evaluation of an Open-Source Python Toolbox for Heart Rate Variability (HRV). *International Conference on Electrical, Electronic and Computing Engineering*

(IcETRAN), 822–828.

Gramfort, A. (2013). MEG and EEG data analysis with MNE-Python. *Frontiers in Neuroscience*, *7*. https://doi.org/10.3389/fnins.2013.00267

Gross, J., Baillet, S., Barnes, G. R., Henson, R. N., Hillebrand, A., Jensen, O., Jerbi, K., Litvak, V., Maess, B., Oostenveld, R., Parkkonen, L., Taylor, J. R., van Wassenhove, V., Wibral, M., & Schoffelen, J.-M. (2013). Good practice for conducting and reporting MEG research. *NeuroImage*, *65*, 349–363. https://doi.org/10.1016/j.neuroimage.2012.10.001

Haapaniemi, T. H. (2001). Ambulatory ECG and analysis of heart rate variability in Parkinson's disease. *Journal of Neurology, Neurosurgery & Psychiatry*, *70*(3), 305–310. https://doi.org/10.1136/jnnp.70.3.305

Haenschel, C., Bittner, R. A., Haertling, F., Rotarska-Jagiela, A., Maurer, K., Singer, W., & Linden, D. E. J. (2007). Contribution of Impaired Early-Stage Visual Processing to Working Memory Dysfunction in Adolescents With Schizophrenia: A Study With Event-Related Potentials and Functional Magnetic Resonance Imaging. *Archives of General Psychiatry*, *64*(11), 1229. https://doi.org/10.1001/archpsyc.64.11.1229

He, B. J. (2014). Scale-free brain activity: Past, present, and future. *Trends in Cognitive Sciences*, *18*(9), 480–487. https://doi.org/10.1016/j.tics.2014.04.003

He, B. J., Zempel, J. M., Snyder, A. Z., & Raichle, M. E. (2010). The Temporal Structures and Functional Significance of Scale-free Brain Activity. *Neuron*, *66*(3), 353–369. https://doi.org/10.1016/j.neuron.2010.04.020

Hunt, A. C. (2002). T Wave Alternans in high arrhythmic risk patients: Analysis in time and frequency domains: A pilot study. *BMC Cardiovascular Disorders*, *2*(1), 6. https://doi.org/10.1186/1471-2261-2-6

Hyvarinen, A. (1999). Fast and robust fixed-point algorithms for independent component

analysis. *IEEE Transactions on Neural Networks*, *10*(3), 626–634. https://doi.org/10.1109/72.761722

Jousmäki, V., & Hari, R. (1996). Cardiac Artifacts in Magnetoencephalogram: *Journal of Clinical Neurophysiology*, *13*(2), 172–176. https://doi.org/10.1097/00004691-199603000-00008

Kanaya, N., Hirata, N., Kurosawa, S., Nakayama, M., & Namiki, A. (2003). Differential Effects of Propofol and Sevoflurane on Heart Rate Variability. *Anesthesiology*, *98*(1), 34–40. https://doi.org/10.1097/00000542-200301000-00009

Kern, M., Aertsen, A., Schulze-Bonhage, A., & Ball, T. (2013). Heart cycle-related effects on event-related potentials, spectral power changes, and connectivity patterns in the human ECoG. *NeuroImage*, *81*, 178–190. https://doi.org/10.1016/j.neuroimage.2013.05.042

Lalor, E. C., Pearlmutter, B. A., Reilly, R. B., McDarby, G., & Foxe, J. J. (2006). The VESPA: A method for the rapid estimation of a visual evoked potential. *NeuroImage*, *32*(4), 1549–1561. https://doi.org/10.1016/j.neuroimage.2006.05.054

Lendner, J. D., Helfrich, R. F., Mander, B. A., Romundstad, L., Lin, J. J., Walker, M. P., Larsson, P. G., & Knight, R. T. (2020). An electrophysiological marker of arousal level in humans. *ELife*, *9*, e55092. https://doi.org/10.7554/eLife.55092

Merkin, A., Sghirripa, S., Graetz, L., Smith, A. E., Hordacre, B., Harris, R., Pitcher, J., Semmler, J., Rogasch, N. C., & Goldsworthy, M. (2022). Do age-related differences in aperiodic neural activity explain differences in resting EEG alpha? *Neurobiology of Aging*, S0197458022002019. https://doi.org/10.1016/j.neurobiolaging.2022.09.003

Miller, K. J., Sorensen, L. B., Ojemann, J. G., & den Nijs, M. (2009). Power-Law Scaling in the Brain Surface Electric Potential. *PLoS Computational Biology*, *5*(12), e1000609. https://doi.org/10.1371/journal.pcbi.1000609

Mitra, P. P., & Pesaran, B. (1999). Analysis of Dynamic Brain Imaging Data. *Biophysical Journal*, *76*(2), 691–708. https://doi.org/10.1016/S0006-3495(99)77236-X

Mostile, G., Giuliano, L., Dibilio, V., Luca, A., Cicero, C. E., Sofia, V., Nicoletti, A., & Zappia, M. (2019). Complexity of electrocortical activity as potential biomarker in untreated Parkinson's disease. *Journal of Neural Transmission*, *126*(2), 167–172. https://doi.org/10.1007/s00702-018-1961-6

Pearson, K. (1901). LIII. On lines and planes of closest fit to systems of points in space. *The London, Edinburgh, and Dublin Philosophical Magazine and Journal of Science*, *2*(11), 559–572. https://doi.org/10.1080/14786440109462720

Penzel, T., Kantelhardt, J. W., Lo, C.-C., Voigt, K., & Vogelmeier, C. (2003). Dynamics of Heart Rate and Sleep Stages in Normals and Patients with Sleep Apnea. *Neuropsychopharmacology*, *28*(S1), S48–S53. https://doi.org/10.1038/sj.npp.1300146

Pritchard, W. S. (1992). The Brain in Fractal Time: 1/F-Like Power Spectrum Scaling of the Human Electroencephalogram. *International Journal of Neuroscience*, *66*(1–2), 119–129. https://doi.org/10.3109/00207459208999796

Salvatier, J., Wiecki, T. V., & Fonnesbeck, C. (2016). Probabilistic programming in Python using PyMC3. *PeerJ Computer Science*, *2*, e55. https://doi.org/10.7717/peerj-cs.55

Saul, J. P., Albrecht, P., Berger, R. D., & Cohen, R. J. (1988). Analysis of long term heart rate variability: Methods, 1/f scaling and implications. *Computers in Cardiology*, *14*, 419–422.

Schmidt, F., Chen, Y.-P., Keitel, A., Rösch, S., Hannemann, R., Serman, M., Hauswald, A., & Weisz, N. (2021). *Neural speech tracking shifts from the syllabic to the modulation rate of speech as intelligibility decreases* [Preprint]. Neuroscience. https://doi.org/10.1101/2021.03.25.437033

Schulz, S. M. (2016). Neural correlates of heart-focused interoception: A functional magnetic resonance imaging meta-analysis. *Philosophical Transactions of the Royal Society B: Biological Sciences*, *371*(1708), 20160018. https://doi.org/10.1098/rstb.2016.0018

Schumann, A., & Bär, K. (2021). *Autonomic Aging: A dataset to quantify changes of cardiovascular autonomic function during healthy aging* (1.0.0) [Data set]. PhysioNet. https://doi.org/10.13026/2HSY-T491

Shaffer, F., & Ginsberg, J. P. (2017). An Overview of Heart Rate Variability Metrics and Norms. *Frontiers in Public Health*, *5*, 258. https://doi.org/10.3389/fpubh.2017.00258

Shafto, M. A., Tyler, L. K., Dixon, M., Taylor, J. R., Rowe, J. B., Cusack, R., Calder, A. J., Marslen-Wilson, W. D., Duncan, J., Dalgleish, T., Henson, R. N., Brayne, C., & Matthews, F. E. (2014). The Cambridge Centre for Ageing and Neuroscience (Cam-CAN) study protocol: A cross-sectional, lifespan, multidisciplinary examination of healthy cognitive ageing. *BMC Neurology*, *14*(1), 204. https://doi.org/10.1186/s12883-014-0204-1

Takarada-Iemata, M., Westenskow, P. D., & Muramatsu, R. (2019). Neurovascular interaction. *Neurochemistry International*, *129*, 104506. https://doi.org/10.1016/j.neuint.2019.104506

Task Force of the European Society of Cardiology the North American Society of Pacing Electrophysiology. (1996). Heart Rate Variability: Standards of Measurement, Physiological Interpretation, and Clinical Use. *Circulation*, *93*(5), 1043–1065. https://doi.org/10.1161/01.CIR.93.5.1043

Taulu, S., & Kajola, M. (2005). Presentation of electromagnetic multichannel data: The signal space separation method. *Journal of Applied Physics*, *97*(12), 124905. https://doi.org/10.1063/1.1935742

Taulu, S., & Simola, J. (2006). Spatiotemporal signal space separation method for rejecting nearby interference in MEG measurements. *Physics in Medicine and Biology*, *51*(7), 1759–1768. https://doi.org/10.1088/0031-9155/51/7/008

Taylor, J. R., Williams, N., Cusack, R., Auer, T., Shafto, M. A., Dixon, M., Tyler, L. K., Cam-CAN, & Henson, R. N. (2017). The Cambridge Centre for Ageing and Neuroscience (Cam-CAN) data repository: Structural and functional MRI, MEG, and cognitive data from a cross-sectional adult lifespan sample. *NeuroImage*, *144*, 262–269. https://doi.org/10.1016/j.neuroimage.2015.09.018

Tsvetanov, K. A., Henson, R. N. A., Tyler, L. K., Davis, S. W., Shafto, M. A., Taylor, J. R., Williams, N., Cam-CAN, & Rowe, J. B. (2015). The effect of ageing on fMRI: Correction for the confounding effects of vascular reactivity evaluated by joint fMRI and MEG in 335 adults. *Human Brain Mapping*, *36*(6), 2248–2269. https://doi.org/10.1002/hbm.22768

Vehtari, A., Gelman, A., Simpson, D., Carpenter, B., & Bürkner, P.-C. (2021). Rank-Normalization, Folding, and Localization: An Improved R̂ for Assessing Convergence of MCMC (with Discussion). *Bayesian Analysis*, *16*(2). https://doi.org/10.1214/20-BA1221

von Rosenberg, W., Chanwimalueang, T., Goverdovsky, V., Peters, N. S., Papavassiliou, C., & Mandic, D. P. (2017). Hearables: Feasibility of recording cardiac rhythms from head and in-ear locations. *Royal Society Open Science*, *4*(11), 171214. https://doi.org/10.1098/rsos.171214

Voytek, B., Kramer, M. A., Case, J., Lepage, K. Q., Tempesta, Z. R., Knight, R. T., & Gazzaley, A. (2015). Age-Related Changes in 1/f Neural Electrophysiological Noise. *Journal of Neuroscience*, *35*(38), 13257–13265. https://doi.org/10.1523/JNEUROSCI.2332-14.2015

Waschke, L., Donoghue, T., Fiedler, L., Smith, S., Garrett, D. D., Voytek, B., & Obleser, J. (2021). Modality-specific tracking of attention and sensory statistics in the human electrophysiological spectral exponent. *ELife*, *10*, e70068. https://doi.org/10.7554/eLife.70068

Welch, P. (1967). The use of fast Fourier transform for the estimation of power spectra: A method based on time averaging over short, modified periodograms. *IEEE Transactions on Audio and Electroacoustics*, *15*(2), 70–73. https://doi.org/10.1109/TAU.1967.1161901

Wen, H., & Liu, Z. (2016). Separating Fractal and Oscillatory Components in the Power Spectrum of Neurophysiological Signal. *Brain Topography*, *29*(1), 13–26. https://doi.org/10.1007/s10548-015-0448-0